An Optimal Scenario-Based Scheduling Method for an SOP-included Active Distribution Network Considering Uncertainty of Load and Renewable Generations

Pezhman Khalouie[1], Payam Alemi[1, *], Mojtaba Beiraghi[1]

[1] *Department of Electrical Engineering, Urmia Branch, Islamic Azad University, Urmia, Iran. Phone Number: +9844331803000, mobile number:+989141802342*

Pezhman.Khalouie@iaurmia.ac.ir, P.Alemi@iaurmia.ac.ir, Beiraghi@iaurmia.edu

[*] *Corresponding author.*

Abstract- The high penetration of renewable Distributed Generators (DGs) in the Active Distribution Network (ADN) in addition to its advantages brings great challenges for the ADN, due to their intermittent and uncertain generations. Increasing network flexibility using Soft Open Points (SOPs) is an effective solution to overcome these challenges. However, an SOP-based ADN may contain various renewable or Controllable DGs (CDGs), and autonomous interconnected Microgrids (MGs). Accordingly, the uncertainty of load and renewable generation makes its scheduling more complex. In this paper, a novel optimal scenario-based framework is proposed to schedule an SOP-included ADN with multi-interconnected microgrids, based on the forecasted scenarios of demand and renewable DGs generation. In the proposed framework, all technical constraints, such as AC load flow equations, SOP's operational limitations, and DG's production range, are modeled in a Second-Order Cone (SOC) programming format. The energy transaction between the ADN and the other agents, i.e., MGs, and Upstream Network (UN) is also considered. This model can be optimally solved in an acceptable time. To show the effectiveness of the proposed method, it is implemented on the IEEE 33-bus distribution network. The simulation results confirm its high accuracy and speed.

Keywords: ADN, SOP, uncertainty, microgrid, renewable DG.

1. Introduction

The high penetration of renewable Distributed Generators (DGs), such as Wind Turbines

(WTs) and Photovoltaics (PVs), exacerbates the uncertainties in the Active Distribution Network (ADN), which makes its scheduling more difficult [1-3]. Various studies such as [4-8] have been presented to determine the optimal scheduling of ADNs or microgrids in the presence of DGs. In [4] an energy management method is proposed for real-time control of a DC microgrid with various types of renewable DGs. The day-ahead scheduling of a microgrid considering the uncertainty of load is presented in [5] using a modified Particle Swarm Optimization (PSO) algorithm. However, the global optimum scheduling is not granted using PSO. In [6], a multi-objective method based on the Harmony Search Algorithm (HSA) is developed for the planning and scheduling of DGs in the ADN. Authors in [7] have developed a bi-level operation model considering the retailers in the upper level and microgrids in the lower level. In this model, microgrids determine the amount of purchasing power from the retailers based on their offered prices which are related to the wholesale market prices. An adaptive fuzzy logic-based energy dispatch is proposed in [8] to consider the inaccurate prediction of the load and renewables generation in the scheduling model. However, the AC load flow equations are not modeled.

To increase the controllability of modern ADNs, Soft Open Points (SOPs) are used in place of normally opened points [9, 10]. The SOP is a flexible power electronic device [11, 12], which can accurately regulate the active and reactive power flow of connected feeders [13, 14]. The SOP can significantly enhance distribution system flexibility and improve voltage regulation of Active Distribution Networks (ADNs) [11]. Also, it can reduce the operational cost of the ADN and improve its performance under the high penetration of renewable resources [9, 15].

Due to the benefits of SOPs in the ADN, some studies such as [15-18] have focused on SOP planning. However, the optimal scheduling of SOPs in the presence of renewable energy resources with intermittent characteristics is a complex problem [19]. Accordingly, a

scheduling model is required to align SOP's operation with the other components in the ADN, i.e., CDGs, renewables DGs, and MGs.

In [9] a decentralized cooperative method for scheduling a multi-area ADN in the presence of inter-area SOPs is proposed. However, the uncertainty of the load and renewable DGs is not considered. Also, financial exchanges between microgrids and ADN are not discussed in the paper.

A multi-time scale robust energy management method for a multiple terminal SOP-based ADN is proposed in [20]. This model cannot deal with the uncertainties of demand and renewable generations in the ADN and only energy exchange fluctuations with MGs are considered. Also, the active and reactive power flow scheduling is modeled separately on two separate levels, which as stated in the results can cause to infeasible solution in some cases.

To coordinate SOPs and DG inverters a universal voltage regulation based on a biconvex model is proposed in [11], which provides local optimum scheduling for an ADN. Nevertheless, the load flow constraints are linearly simplified and SOP losses are not considered.

In [21] a reactive power control method for distribution systems with SOP and direct load control of air-conditioning is formulated in a mixed nonlinear integer model and solved using a parallel cooperative co-evolutionary differential evolution algorithm. However, there is no guarantee that the solution will be the global optimum.

A deterministic day-ahead dispatch model based on long-term forecasts is proposed in [22] to decrease the power loss and promote the consumption of renewable DGs. However, the uncertainties of load and renewable DGs are not considered in the day-ahead scheduling stage.

In [23], using a Jacobian matrix-based sensitivity analysis a non-linear programming optimization is developed, to set the active and reactive power operating set-points for an

SOP. However, for simplicity, the power losses of the SOP are neglected.

In [24], a deterministic multi-objective particle swarm optimization algorithm was proposed to improve the operation of a distribution network with DG and an SOP. Where voltage profile improvement, feeder load balancing, and power loss reduction, were taken as objectives. However, the uncertainties of load and renewable DGs and the SOP's power losses are neglected.

A combined decentralized and local voltage control strategy of SOPs is proposed in [13], which regulates the active power transmission of SOPs. This method can only obtain near-global optimal scheduling results.

Some studies such as [25-28], considered the uncertainty of the load demand, price of power, and renewable generation in the scheduling or planning model. In [25] a robust optimization model is used to depict the uncertainty of the PV generations for SOP and DGs planning. In this model, the worst-case scenario that maximizes system costs is considered the production forecast. This strict risk-averse modeling is not suitable for the short-term scheduling of an SOP-included ADN. Because, in the short term, the prediction of real values is available [27] and there is no need for a worst-case prediction. In [26], the uncertainty of the load, and renewable generation are modeled by a simple exponential smoothing model with random variables. This model can only consider one prediction value of uncertain parameters.

A two-time scale robust approach is proposed in [27] to deal with the uncertainty of the renewable generation in a multi-terminal SOP-included ADN. However, the uncertainty of load demand is neglected. Also, energy transactions between areas are not modeled and only technical aspects such as voltage profile improvement and loss reduction are considered.

A scenario-based planning model is used in [28] to model various scenarios of uncertain parameters, i.e., load demand, and renewable generation. In this method, these scenarios are created randomly. Also, to reduce the computational burden, these scenarios are represented

by their center which is calculated by the k-means clustering method. However, the energy exchange between the ADN and MGs is not considered.

The predicted curves of load demand and renewables generation are required for the day-ahead scheduling of the ADN. For accurate prediction of these values, different frameworks are proposed, such as OS-KRRVFLN in [29], and DANN in [30]. Different forecasting methods lead to different scenarios for uncertain parameters, i.e., load demand and renewable generation curves. To consider these scenarios in the day-ahead scheduling of an SOP-based ADN a fast and optimal approach is required. In this regard, this paper proposes a scenario-based framework, in which its main contributions are as follows:

- A scenario-based model for economic day-ahead scheduling of an SOP-based ADN in the presence of renewables DGs and CDGs is proposed. In this model, active and reactive power dispatch of DERs and SOPs are coordinated, considering both economic and technical aspects.
- The uncertainty of the load and renewables generation is modeled using convex scenario-based stochastic programming.
- Energy transactions between the ADN and its connected MGs and between ADN and its Upstream Network (UN) are considered.
- Both active and reactive transactions with MGs and the UN are integrated into the model and coordinated with SOPs and DERs scheduling.
- Active and reactive power transactions between the ADN, UN, and MGs are settled simultaneously with DERs scheduling, considering all technical constraints such as power flow and voltage limit constraints. This feature ensures the achievement of economic goals while meeting technical constraints.

To highlight the innovations of this paper, the existing scheduling methods are compared with the proposed model in Table 1.

The rest of this manuscript is as follows, the ADN structure is introduced in section 2. The proposed model is proposed in Section 3. Case studies and results are discussed in section 4, and the paper is concluded in section 5.

2. The Active Distribution Network

An ADN is shown in Fig. 1, which contains a local network, some consumers, Distributed Energy Resources (DERs), i.e., WTs, PVs, and CDGs, and two SOPs. As can be seen, some autonomous MGs are connected to the ADN in different buses, and the ADN is connected to the UN through its slack bus.

It is assumed that the UN, the ADN, and each of the MGs are autonomous agents which are operated to increase their profits. The energy trading scheme among these agents is shown in Fig. 2.

As can be seen in this figure, first, the UN sends the wholesale price to the ADN. Then the ADN sends the retail price to the MGs. Each of the MGs schedules its area autonomously based on this retailed price, and sends its quantity of exchanged energy to the ADN. Finally, the ADN calculates the quantity of hourly exchanged energy considering the wholesale price and received quantities of exchanged energy. The proposed model for optimal day-ahead scheduling of the SOP-based ADN in the presence of interconnected MGs, renewable DGs, and CDGs is presented in the next section.

3. The Proposed Optimal Scheduling Model

The focus of this paper is on minimizing the ADN's operation cost, considering the uncertainties of the demand and renewable DGs. Since the exact value of these parameters is unknown when optimal day-ahead scheduling, a new economic scenario-based model is developed.

As the number of scenarios increases, the accuracy of the modeling also increases, however, it imposes a higher computational burden [31]. Consequently, a proper scenario reduction

strategy such as k-means [32], the simultaneous backward technique [33], and a mixed-integer linear optimization method [34], should be applied to the problem. However, in this paper, it is assumed the scenarios of the demand and renewable generations are predefined parameters, and the effect of each scenario is proportional to its probability.

So, the total day-ahead operation cost can be formulated as (1).

$$C_{to} = \sum_{w \in W} r^w C_{to}^w \tag{1}$$

Where w and W are respectively the index and set of demand and renewable generation scenarios, r^w is the probability of scenario w, C_{to} is the ADN's operation cost in the scheduling horizon, and C_{to}^w is the total cost of the ADN in scenario w which is defined in (2).

$$C_{to}^w = C_{UN} + C_{CDG}^w + C_l^w, \forall w \in W \tag{2}$$

Where, C_{UN} is the cost of net imported electrical energy from the UN. C_{CDG}^w is the CDG's operation cost, and C_l^w is the cost of total energy losses in scenario w.

The ADN should determine the quantity of exchanged energy by the UN, based on the received wholesale electricity price. Accordingly, the net imported energy cost from the UN is calculated based on (3).

$$C_{UN} = \sum_{t \in T} \tau \times \lambda_t \times P_{UN,t}, \forall w \in W \tag{3}$$

Where t, T, and τ are respectively index, set, and the length of time intervals. represent the quantity of purchased active power from the UN (exported from the UN to the ADN) in time interval t, λ_t is the per-unit wholesale electricity price in time interval t. As shown in Fig. 2, from the ADN point of view λ_t and the quantity of exchanged energy with the MGs are

predefined parameters that are respectively determined by the UN and the MGs, before the day-ahead scheduling. The retail price of electricity is assumed to be a specific parameter that is concluded based on the trading contract between the MGs and the ADN. Accordingly, the revenue of energy trading between the ADN and the MGs is a fixed term, so it is neglected in C_{to}^{w}.

C_{CDG}^{w} are defined in **Error! Reference source not found.** [35].

$$C_{CDG}^{w} = \sum_{t \in T} \sum_{c \in C} \left(a_c \times Pc_{t,c}^{w\ 2} + b_c \times Pc_{t,c}^{w} + c_c \right) \times \tau, \forall w \in W \tag{4}$$

Where c and C are index and set of CDGs, a_c, b_c, and c_c are cost coefficient of CDG c, $Pc_{t,c}^{w}$ is the active power output of CDG c in scenario w and tth time interval.

The cost of energy losses (C_{l}^{w}) include two separate parts, i.e., branches and SOP's losses. Accordingly, C_{l}^{w} is represented in **Error! Reference source not found.**, where C_{lB}^{w} and C_{lS}^{w} are respectively the cost of total energy losses in the ADN's branches and the SOP's converters [9].

$$C_{l}^{w} = C_{lB}^{w} + C_{lS}^{w}, \forall w \in W \tag{5}$$

These two parts are respectively defined in **Error! Reference source not found.** and **Error! Reference source not found.** [9].

$$C_{lB}^{w} = \sum_{t \in T} \left(\lambda_t \times \tau \sum_{ij \in B} \left(r_{ij} \times I_{t,ij}^{w} \right) \right), \forall w \in W \tag{6}$$

$$C_{lB}^{w} = \sum_{t \in T} \left(\lambda_t \times \tau \sum_{s \in S} \left(Pls_{t,s}^{w} \right) \right), \forall w \in W \tag{7}$$

Where ij and B are respectively the index and set of ADN's branches, r_{ij} is the resistance of branch ij, $I_{t,ij}^{w}$ is the squared current magnitude of branch ij in scenario w and time interval t, s and S are respectively index and set of SOPs, and $Pls_{t,s}^{m}$ is the power loss of SOP s.

According to [9], the power losses of an SOP can be represented by the loss coefficient of its converters using **Error! Reference source not found.**-(11).

$$Pls_{t,s}^{w} = Zl_{s,1}^{w} \times Psm_{t,s,1}^{w} + Zl_{s,2}^{w} \times Psm_{t,s,2}^{w}, \forall t \in T, \forall s \in S, \forall w \in W \quad (8)$$

Where, $Zl_{s,1}^{w}$ and $Zl_{s,2}^{w}$ are the loss coefficients of SOP's converters. $Psm_{t,s,1}^{w}$ and $Psm_{t,s,2}^{m}$ represent the absolute values of injected active power from converter 1 ($Ps_{t,s,1}^{w}$) and convert 2 ($Ps_{t,s,2}^{w}$) of *s*th SOP in time interval *t*. The relation between $Psm_{t,s,1/2}^{w}$ and $Ps_{t,s,1/2}^{w}$, are presented in **Error! Reference source not found.** to **Error! Reference source not found.**, using an inequality constraint.

$$Ps_{t,s,1/2}^{w} \le Psm_{t,s,1/2}^{w}, \forall t \in T, \forall s \in S, \forall w \in W \quad (9)$$

$$-Ps_{t,s,1/2}^{w} \le Psm_{t,s,1/2}^{w}, \forall t \in T, \forall s \in S, \forall w \in W \quad (10)$$

Sop's active power balance is presented in (11).

$$Ps_{t,s,1}^{w} + Ps_{t,s,2}^{w} + Pls_{t,s}^{w} = 0, \forall t \in T, \forall s \in S, \forall w \in W \quad (11)$$

Equations (12) and (13) represent the reactive and apparent power injection threshold of both the SOP converters, respectively.

$$-Qs_{\max,s,1/2} \le Qs_{t,s,1/2}^{w} \le Qs_{\max,s,1/2}, \forall t \in T, \forall s \in S, \forall w \in W \quad (12)$$

$$\left\| Ps_{t,s,1/2}^{w}, Qs_{t,s,1/2}^{w} \right\|_2 \le Ss_{\max,s,1/2}, \forall t \in T, \forall s \in S, \forall w \in W \quad (13)$$

Where $Qs_{\max,s,1/2}$ and $Ss_{max,s,1/2}$ are respectively the maximum reactive and apparent power injection capacity of converters 1/2 SOP *s*.

The maximum value of active, reactive, and apparent power output of CDGs, are expressed in (14) and (15), respectively [36].

$$Pc_{\min,c} \le Pc_{t,c}^{w} \le Pc_{\max,c}, \forall t \in T, \forall c \in C, \forall w \in W \quad (14)$$

$$\left\| Pc_{t,c}^{w}, Qc_{t,c}^{w} \right\|_2 \le Sc_{\max,c}, \forall t \in T, \forall c \in C, \forall w \in W \quad (15)$$

$$-Qc_{\max,t,c}^{w} \le Qc_{t,c}^{w} \le Qc_{\max,t,c}^{w}, \forall t \in T, \forall c \in C, \forall w \in W \quad (16)$$

$$Qc^{w}_{\max,t,c} = Pc^{w}_{t,c} \times \tan\left(\cos^{-1}\left(PF^{CDG}_{\min,c}\right)\right) \quad (17)$$

$Pc_{max,c}/Pc_{min,c}$, and $Sc_{max,c}$ are respectively the maximum/minimum active, and apparent power output of *c*th CDG. $Qc^{w}_{max,t,c}$ is the maximum reactive power capacity of CDG *c* in scenario *w* and time interval *t*, and $PF^{CDG}_{min,c}$ is the minimum Power Factor (PF) of CDG *c*. Equations (16) and (17) limit the reactive power generation or absorption of CDGs based on the minimum PF of the CDGs.

In the proposed scenario-based scheduling framework, the AC load flow constraints are represented using the *DistFlow* model [37]. The effect of SOP on the ADN's power flow is graphically illustrated in Fig. 3.

In this figure, injected powers to bus *j* are drawn with red color, while exported powers from it are drawn with green. Also, the net injected active and reactive power to bus *j* from its connected DERs are respectively indicated by $Pn^{w}_{t,j}$ and $Qn^{w}_{t,j}$. These by $Pn^{w}_{t,j}$ and $Qn^{w}_{t,j}$. These variables are defined in equations (18) and (19).

$$Pn^{w}_{t,j} = \sum_{p \in PV_j} Pp^{w}_{t,p} + \sum_{v \in WT_j} Pw^{w}_{t,v} + \sum_{c \in C_j} Pc^{w}_{t,c}, \forall t \in T, \forall j \in N, \forall w \in W \quad (18)$$

$$Qn^{w}_{t,j} = \sum_{c \in C_j} Qc^{w}_{t,c}, \forall t \in T, \forall j \in N, \forall w \in W \quad (19)$$

$Pp^{w}_{t,p}$ and $Pw^{w}_{t,v}$ are respectively the generation value of *p*th PV and *v*th WT in scenario *w* and in time interval *t*. PV_j, WT_j, and C_j are respectively the set of installed PVs, WTs, and CDGs in bus *j*.

$Ps^{w}_{t,j}$ and $Qs^{w}_{t,j}$ are respectively the net injected active and reactive power from SOPs to bus *j* which are represented in **Error! Reference source not found.** and **Error! Reference source not found.**.

$$Ps^{w}_{t,j} = \sum_{s \in S_{1,j}} Ps^{w}_{t,s,1} + \sum_{s \in S_{2,j}} Ps^{w}_{t,s,2}, \forall t \in T, \forall j \in N, \forall w \in W \quad (20)$$

$$Qs_{t,j}^{w} = \sum_{s \in S_{1,j}} Qs_{t,s,1}^{w} + \sum_{s \in S_{2,j}} Qs_{t,s,2}^{w}, \forall t \in T, \forall j \in N, \forall w \in W \quad (21)$$

Where $S_{1/2,j}$ is the set of SOPs that are directly connected to bus *j* through converter 1/2. In the proposed framework, the active and reactive power equilibrium constraints are represented by (22) and (23), respectively.

$$Pi_{t,ij}^{w} + Ps_{t,j}^{w} + Pn_{t,j}^{w} - Pl_{t,j}^{w} + P_{UN,t,j} - \sum_{m \in M_j} P_{MG,m} = \sum_{k \in Dn_j} Pb_{t,jk}^{w}, \forall t \in T, \forall j \in N, \forall w \in W \quad (22)$$

$$Qi_{t,ij}^{w} + Qs_{t,j}^{w} + Qn_{t,j}^{w} - Ql_{t,j}^{w} + Q_{UN,t,j} - \sum_{m \in M_j} Q_{MG,m} = \sum_{k \in Dn_j} Qb_{t,jk}^{w}, \forall t \in T, \forall j \in N, \forall w \in W \quad (23)$$

Where $Pl_{t,j}^{w}$ and $Ql_{t,j}^{w}$ are respectively the active and reactive power demand of bus *j* in the t th interval and w th scenario. The set of downstream buses of bus *j* is indicated by Dn_j. N is the set of all the buses in the ADN. Also, M_j is the set of interconnected MGs to bus *j*, and *m* is the index of MGs. $P_{MG,m}$ and $Q_{MG,m}$ are the exported active and reactive power to MG *m*, respectively. $Pb_{t,jk}^{w}$ is the injected active power to branch *jk* from its sending-end (bus *j*) in *t*th interval and scenario *w*, while $Qb_{t,jk}^{w}$ is the injected reactive powers to it. $P_{UN,t,j}$ and $Q_{UN,t,j}$ are the injected active and reactive powers to bus *j* from the UN, in *t*th time interval, respectively. $Pi_{t,ij}^{w}$ and $Qi_{t,ij}^{m}$ are the net injected active and reactive powers to the receiving end of branch ij (bus *j*) which are respectively defined in (24) and (25).

$$Pi_{t,ij}^{w} = Pb_{t,ij}^{w} - r_{ij} \times I_{t,ij}^{w}, \forall t \in T, \forall ij \in B, \forall w \in W \quad (24)$$

$$Qi_{t,ij}^{w} = Qb_{t,ij}^{w} - x_{ij} \times I_{t,ij}^{w}, \forall t \in T, \forall ij \in B, \forall w \in W \quad (25)$$

$I_{t,ij}^{w}$ is the squared current magnitude of branch ij, in *t*th time interval in scenario *w*. r_{ij} and x_{ij} are respectively the resistance and reactance of branch ij.

Ohm's law is expressed in (26), and the branch's equation, i.e., $v_{t,i}^{w} \times I_{t,ij}^{w} = Pb_{t,ij}^{w\,2} + Qb_{t,ij}^{w\,2}$ is represented by inequality (27) in the Second-Order Cone (SOC) form [35].

$$v_{t,j}^{w} = v_{t,i}^{w} - 2\left(r_{ij} \times Pb_{t,ij}^{w} + x_{ij} \times Qb_{t,ij}^{w}\right) + I_{t,ij}^{w} \times \left(r_{ij}^{2} + x_{ij}^{2}\right), \forall t \in T, \forall ij \in B, \forall w \in W \quad (26)$$

$$\left\| \begin{bmatrix} 2Pb_{t,ij}^{w} \\ 2Qb_{t,ij}^{w} \\ I_{t,ij}^{w} - v_{t,ij}^{w} \end{bmatrix} \right\|_2 \leq v_{t,i}^{w} + I_{t,ij}^{w}, \forall t \in T, \forall ij \in B, \forall w \in W \quad (27)$$

Where $v_{t,j}^{w}$ represent the square voltage amplitude of bus *j*, and $\|A\|_2$ represents 2-norm of vector *A*.

Constraint (28) limits the maximum current of branches, where $I_{max,ij}^{m}$ represent the maximum allowed squared current amplitude of branch *ij*.

$$0 \leq I_{t,ij}^{w} \leq I_{ij}^{\max}, \forall t \in T, \forall ij \in B, \forall w \in W \quad (28)$$

Constraints (29) and (30) enforce the allowed nodal voltage limits of the ADN's buses. In these equations, v_{min} and v_{max} are respectively the minimum and maximum squared voltage magnitude ofhe buses. v_{sl} and N_{sl} are respectively the nodal voltage amplitude, and the set of slack bus in the ADN.

$$v_{\min}^{2} \leq v_{t,j}^{w} \leq v_{\max}^{2}, \forall t \in T, \forall j \in N, \forall w \in W \quad (29)$$

$$v_{t,j}^{w} = v_{sl}^{2}, \forall t \in T, \forall j \in N_{sl}, \forall w \in W \quad (30)$$

The imported apparent and active powers from the UN are respectively limited in (31) and (32).

$$\left\| P_{UN,t,j}, Q_{UN,t,j} \right\|_2 \leq S_{UN,j}^{\max}, \forall t \in T, \forall j \in N \quad (31)$$

$$-S_{UN,j}^{\max} \leq P_{UN,t,j} \leq S_{UN,j}^{\max}, \forall t \in T, \forall j \in N, \forall w \in W \quad (32)$$

Where, $S_{UN,j}^{max}$ is the maximum allowed imported apparent power from the UN to bus *j*. The imported reactive power from the UN is limited based on the minimum allowed PF in (33) and (34).

$$-Q_{UN,t,j}^{\max} \leq Q_{UN,t,j}^{w} \leq Q_{UN,t,j}^{\max}, \forall t \in T, \forall j \in N, \forall w \in W \quad (33)$$

$$Q_{UN,j}^{\max} = Pm_{UN,t,j} \times \tan\left(\cos^{-1}\left(PF_{\min,j}^{UN}\right)\right), \forall t \in T, \forall j \in N, \forall w \in W \quad (34)$$

$$P_{UN,t,j} \le Pm_{UN,t,j}, \forall t \in T, \forall j \in N, \forall w \in W \quad (35)$$

$$-P_{UN,t,j} \le Pm_{UN,t,j}, \forall t \in T, \forall j \in N, \forall w \in W \quad (36)$$

Where, $Q_{UN,t,j}^{max}$ is the maximum value of exchanged reactive power between the UN and bus j in tth time interval, and $PF_{min,j}^{UN}$ is the smallest allowed PF of imported power from the UN to bus j. $Pm_{UN,t,j}$ represents the absolute value of $P_{UN,t,j}$ and is defined using (35) and (36).

Finally, the proposed scenario-based framework for day-ahead scheduling of the SOP-based ADN is represented in a compact form in (37).

$$\min \sum_{m \in N_m} C_{to} \quad (37)$$
Subject to (2)-(30)

The proposed scenario-based model in (37) is a SOC programming in which the optimality of such optimization problems has already been proven mathematically in [38] and [39].

4. Simulation results

To evaluate the accuracy and solution speed of the proposed framework, it is implemented in the modified IEEE 33-bus distribution network with 4 interconnected MGs and 2 SOPs. The simulations were performed using YALMIP [40] in MATLAB R2020b. Since the proposed model is formulated in the SOC programming format, it can easily be solved by the MOSEK on an ordinary personal computer, and reach the global optimum. Note, the simulations were carried out on a personal laptop with the Intel® Core™ i5-3210M (2.5 GHz) processor, and only 4 GB of RAM.

4.1. The modified IEEE 33-bus

This ADN consists of 33 buses, 32 branches, 2 SOPs, and 4 MGs, i.e., MG_1 to MG_4 which are respectively connected to buses 12, 16, 21, and 23. As shown in Fig. 4, the SOPs are plotted by dashed lines, and the ADN is connected to the UN through its slack bus, i.e., bus 1.

Branche's data, and the detailed data of the CDGs, and SOPs are extracted from [9]. However, to increase the penetration level of the renewable DGs, the nominal power of WTs and PVs has been tenfold. The rated capacity of renewable DGs in this ADN is given in Table 2.

In this ADN, 4 scenarios of demand and renewable generations with the same probability are considered. The forecasted load demands, along with the forecasted production of the PV and WT are shown in Fig. 5 (a) to (b). Note, how to calculate these scenarios is not in the scope of this paper. However, it assumed that these predicted scenarios are the output of effective prediction methods such as [29] and [30].

The wholesale electricity price in the scheduling horizon, which is announced by the UN, is shown in Fig. 6. The quantity of exported electrical energy from the ADN to the MGs is shown in Fig. 7. Note these quantities are offered by the MGs, so they are predefined parameters from the ADN point of view.

4.2. Scheduling results in the presence of SOPs

The proposed scheduling model is a SOC programming that has a high solution speed. The proposed scheduling model for this ADN has been solved using the interior-point method in the MOSEK only after 27 iterations within 1.6092 seconds.

The hourly variations of the voltage amplitude of all 33 buses are shown in Fig. 8. As can be seen, in all scenarios, all the voltage magnitudes are within the predefined range, i.e., [0.95 1.05] pu.

The hourly current magnitude of all branches in all scenarios is shown in Fig. 9. This figure confirms that these currents are less than the maximum predefined threshold (1 pu). Accordingly, the proposed method satisfies the maximum capacity of the branches.

The energy losses of this ADN in all scenarios are given in Table 3.

As can be seen in this table, the share of SOP's power losses in scenarios 1 to 4 is

respectively 21.81, 27.96, 28.23, and 34.73 percent. Accordingly, the power losses of the SOP should be considered in the scheduling.

The hourly operational scheduling of SOPs in scenarios 1, 2, 3, and 4 are respectively shown in Fig. 10, Fig. 11, Fig. 12, and Fig. 13.

According to these figures, the proposed model successfully satisfies all technical operation constraints of SOPs, i.e., maximum capacity and the active power balance constraint in all the scenarios.

To check the accuracy of the SOC relaxation in constraint (27), the AC load flow results are listed in Table 4, and the maximum hourly error of the SOC relaxation is shown in Fig. 14.

According to Fig. 14, the maximum SOC relaxation error is less than 5×10^{-6} pu. These results confirm the high accuracy of the proposed scheduling model from the viewpoint of AC load flow constraints.

To compare the share of each CDG in total CDG generation, the share of each CDG is shown in Fig. 15. As can be seen in this figure, CDGs 8 and 9 have the highest share, because their production costs are the lowest.

Examination of the CDG's scheduling results shows the maximum generation threshold along with the smallest PF constraints in equations (14) to (17) have been met in all scenarios. For instance, the CDG's operation scheduling in scenario 1 is shown in Fig. 16. As can be seen, both economic and technical aspects have been met simultaneously in the obtained results.

The injected active and reactive power to bus 1 from the UN are respectively shown in Fig. 17 (a) and (b). In this ADN, the minimum PF of imported power from the UN is set to 0.8, i.e., $PF_{min,j}^{UN}=0.8$. Examination of the exchanged power between the ADN and the UN shows that the capacity constraint and the minimum PF constraints, i.e., constraints (31) to (36) have been met. As shown in part (a), $Pm_{UN,t,1}$ is equal to the absolute value of $P_{UN,t,1}$, which confirms the accuracy of the model.

In Fig. 18, the total CDGs, WT and PV generation, total imported energy from the UN, along with total load, total power losses, and quantity of exported energy to the MGs are compared in all the scenarios. As expected, the net imported energy from the UN is the same in all the scenarios. Accordingly, using the proposed method, the ADN's operator can determine the optimal quantity of imported energy from the UN based on all possible scenarios of demand and renewable generation.

The details of the operating costs in each scenario are listed in Table 5. In this ADN, since the penetration of renewables is high, the net imported energy from the UN is negative.

In scenario 1, the operational cost is negative (C_{to}^{w}), this means that the revenue from selling energy to the UN is bigger than other operational costs. Note, the total operation cost (C_{to}) of the ADN is 3235.4462 $.

4.3. Compair of results

To investigate the effect of SOPs in reducing the scheduling cost of the ADN, the operational scheduling of the ADN without SOPs has also been performed. In this case, all data is the same as the SOP-included ADN in the last section, only the minimum allowed imported power factor from the UN has been reduced to 0.5 ($PF_{min,j}^{UN} = 0.5$), due to the reduction of reactive power generation capacity of the ADN in this case. The operational cost of the ADN, in this case, is given in Table 6.

As shown in this table, the cost of power losses and the cost of CDGs without SOPs are smaller than the case with SOPs. However, ADN's net income from selling power to the UN in the percent of SOP is 9273.87 $ which is higher than 470 % from the case without SOP (1972.09 $). Also, net costs of the SOP-included ADN in all scenarios are significantly lower than without SOPs. The average cost of the SOP-included ADN is 3235.4462 $ which is significantly smaller than the case without SOPs (7977.1527 $). According to these results, in the presence of SOPs, CDG generation can increase. In this situation, the ADN earns more

income by selling its excess generation to the UN.

5. Conclusion

In this paper, the optimal scheduling of an SOP-based ADN with multi-interconnected MGs is obtained, using various scenarios of demand and renewable generation. The proposed method is formulated as a SOC programming problem. The effectiveness of the proposed method has been evaluated on the modified IEEE 33-bus distribution network, with 4 interconnected MGs, considering 4 different scenarios of the demand and renewable generation. The CPU time of the proposed scenario-based method is less than 2 seconds, which shows the high-speed nature of the proposed method. According to the simulation result, all technical constraints such as AC load flow constraints, CDGs, and SOPs operational constraints are precisely modeled. The scheduling of the CDGs, SOPs, and exchanged power with the UN are economically coordinated, according to the hourly exchanged energy with the MGs.

References

[1] Li P., Wang Y., Ji H. *et al.*, "Operational flexibility of active distribution networks: Definition, quantified calculation and application", *International Journal of Electrical Power & Energy Systems*, 119(pp. 105872 (2020).

[2] Xie Y., Liu L., Wu Q. *et al.*, "Robust model predictive control based voltage regulation method for a distribution system with renewable energy sources and energy storage systems", *International Journal of Electrical Power & Energy Systems*, 118(pp. 105749 (2020).

[3] Korab R., Połomski M., and Owczarek R., "Application of particle swarm optimization for optimal setting of Phase Shifting Transformers to minimize unscheduled active power flows", *Applied Soft Computing*, 105(pp. 107243 (2021).

[4] Rajasekaran R. and Usha Rani P., "Combined HCS–RBFNN for energy management of multiple interconnected microgrids via bidirectional DC–DC converters", *Applied Soft Computing*, 99(pp. 106901 (2021).

[5] Gholami K. and Dehnavi E., "A modified particle swarm optimization algorithm for scheduling renewable generation in a micro-grid under load uncertainty", *Applied Soft Computing*, 78(pp. 496-514 (2019).

[6] S K. and D.M V. K., "Optimal planning of active distribution networks with hybrid distributed energy resources using grid-based multi-objective harmony search algorithm", *Applied Soft Computing*, 67(pp. 387-398 (2018).

[7] Fateh H., Bahramara S., and Safari A., "Modeling operation problem of active distribution networks with retailers and microgrids: A multi-objective bi-level approach", *Applied Soft Computing*, 94(pp. 106484 (2020).

[8] Dong W., Yang Q., Fang X. *et al.*, "Adaptive optimal fuzzy logic based energy management in multi-energy microgrid considering operational uncertainties", *Applied Soft Computing*, 98(pp. 106882 (2021).
[9] Bastami H., Shakarami M. R., and Doostizadeh M., "A decentralized cooperative framework for multi-area active distribution network in presence of inter-area soft open points", *Applied Energy*, 300(pp. 117416 (2021).
[10] Aithal A., Li G., Wu J. *et al.*, "Performance of an electrical distribution network with Soft Open Point during a grid side AC fault", *Applied Energy*, 227(pp. 262-272 (2018).
[11] Zheng Y., Song Y., and Hill D. J., "A general coordinated voltage regulation method in distribution networks with soft open points", *International Journal of Electrical Power & Energy Systems*, 116(pp. 105571 (2020).
[12] Cao W., Wu J., Jenkins N. *et al.*, "Operating principle of Soft Open Points for electrical distribution network operation", *Applied Energy*, 164(pp. 245-257 (2016).
[13] Li P., Ji H., Yu H. *et al.*, "Combined decentralized and local voltage control strategy of soft open points in active distribution networks", *Applied Energy*, 241(pp. 613-624 (2019).
[14] Ding T., Wang Z., Jia W. *et al.*, "Multiperiod Distribution System Restoration With Routing Repair Crews, Mobile Electric Vehicles, and Soft-Open-Point Networked Microgrids", *IEEE Transactions on Smart Grid*, 11(6), pp. 4795-4808 (2020).
[15] Zhang J., Foley A., and Wang S., "Optimal planning of a soft open point in a distribution network subject to typhoons", *International Journal of Electrical Power & Energy Systems*, 129(pp. 106839 (2021).
[16] Qin Q., Han B., Li G. *et al.*, "Capacity allocations of SOPs considering distribution network resilience through elastic models", *International Journal of Electrical Power & Energy Systems*, 134(pp. 107371 (2022).
[17] Wang C., Song G., Li P. *et al.*, "Optimal siting and sizing of soft open points in active electrical distribution networks", *Applied Energy*, 189(pp. 301-309 (2017).
[18] Zhang L., Shen C., Chen Y. *et al.*, "Coordinated allocation of distributed generation, capacitor banks and soft open points in active distribution networks considering dispatching results", *Applied Energy*, 231(pp. 1122-1131 (2018).
[19] Li B., Liang Y., Wang G. *et al.*, "A control strategy for soft open points based on adaptive voltage droop outer-loop control and sliding mode inner-loop control with feedback linearization", *International Journal of Electrical Power & Energy Systems*, 122(pp. 106205 (2020).
[20] Sun F., Yu M., Wu Q. *et al.*, "A multi-time scale energy management method for active distribution networks with multiple terminal soft open point", *International Journal of Electrical Power & Energy Systems*, 128(pp. 106767 (2021).
[21] Wang Q., Liao J., Su Y. *et al.*, "An optimal reactive power control method for distribution network with soft normally-open points and controlled air-conditioning loads", *International Journal of Electrical Power & Energy Systems*, 103(pp. 421-430 (2018).
[22] Zhu J., Yuan Y., and Wang W., "Multi-stage active management of renewable-rich power distribution network to promote the renewable energy consumption and mitigate the system uncertainty", *International Journal of Electrical Power & Energy Systems*, 111(pp. 436-446 (2019).
[23] Long C., Wu J., Thomas L. *et al.*, "Optimal operation of soft open points in medium voltage electrical distribution networks with distributed generation", *Applied Energy*, 184(pp. 427-437 (2016).
[24] Qi Q., Wu J., and Long C., "Multi-objective operation optimization of an electrical

distribution network with soft open point", *Applied Energy*, 208(pp. 734-744 (2017).
[25] Zhang T., Wang J., Zhong H. *et al.*, "Soft Open Point Planning in Renewable-dominated Distribution Grids with Building Thermal Storage", *CSEE Journal of Power and Energy Systems*, 9(1), pp. 244-253 (2023).
[26] Yang X., Song Z., Wen J. *et al.*, "Network-Constrained Transactive Control for Multi-Microgrids-based Distribution Networks with SOPs," p. arXiv:2011.03163doi: 10.48550/arXiv.2011.03163.
[27] Sun F., Ma J., Yu M. *et al.*, "Optimized Two-Time Scale Robust Dispatching Method for the Multi-Terminal Soft Open Point in Unbalanced Active Distribution Networks", *IEEE Transactions on Sustainable Energy*, 12(1), pp. 587-598 (2021).
[28] Wang J., Zhou N., Chung C. Y. *et al.*, "Coordinated Planning of Converter-Based DG Units and Soft Open Points Incorporating Active Management in Unbalanced Distribution Networks", *IEEE Transactions on Sustainable Energy*, 11(3), pp. 2015-2027 (2020).
[29] Majumder I., Dash P. K., and Dhar S., "Real-time Energy Management for PV–battery–wind based microgrid using on-line sequential Kernel Based Robust Random Vector Functional Link Network", *Applied Soft Computing*, 101(pp. 107059 (2021).
[30] Masoumi A., Ghassem-zadeh S., Hosseini S. H. *et al.*, "Application of neural network and weighted improved PSO for uncertainty modeling and optimal allocating of renewable energies along with battery energy storage", *Applied Soft Computing*, 88(pp. 105979 (2020).
[31] Sedighizadeh M., Esmaili M., Jamshidi A. *et al.*, "Stochastic multi-objective economic-environmental energy and reserve scheduling of microgrids considering battery energy storage system", *International Journal of Electrical Power & Energy Systems*, 106(pp. 1-16 (2019).
[32] Sachs J. and Sawodny O., "Multi-objective three stage design optimization for island microgrids", *Applied Energy*, 165(pp. 789-800 (2016).
[33] Kim H. J. and Kim M. K., "Risk-based hybrid energy management with developing bidding strategy and advanced demand response of grid-connected microgrid based on stochastic/information gap decision theory", *International Journal of Electrical Power & Energy Systems*, 131(pp. 107046 (2021).
[34] Karimi H., Bahmani R., and Jadid S., "Stochastic multi-objective optimization to design optimal transactive pricing for dynamic demand response programs: A bi-level fuzzy approach", *International Journal of Electrical Power & Energy Systems*, 125(pp. 106487 (2021).
[35] Bastami H., Shakarami M. R., and Doostizadeh M., "A non-hierarchical ATC framework for parallel scheduling of active distribution network with multiple autonomous microgrids", *International Journal of Electrical Power & Energy Systems*, 133(pp. 107293 (2021).
[36] Wang J., Zhou N., and Wang Q., "Data-driven stochastic service restoration in unbalanced active distribution networks with multi-terminal soft open points", *International Journal of Electrical Power & Energy Systems*, 121(pp. 106069 (2020).
[37] Doostizadeh M., Shakarami M. R., and Bastami H., "Decentralized energy trading framework for active distribution networks with multiple microgrids under uncertainty(Invited Paper)", *Scientia Iranica*, 26(Special Issue on machine learning, data analytics, and advanced optimization techniques in modern power systems [Transactions on Computer Science & Engineering and Electrical Engineering(D)]), pp. 3606-3621 (2019).
[38] Farivar M. and Low S. H., "Branch Flow Model: Relaxations and Convexification—Part I", *IEEE Transactions on Power Systems*, 28(3), pp. 2554-2564 (2013).

[39] Nick M., Cherkaoui R., Boudec J. L. *et al.*, "An Exact Convex Formulation of the Optimal Power Flow in Radial Distribution Networks Including Transverse Components", *IEEE Transactions on Automatic Control,* 63(3), pp. 682-697 (2018).
[40] Lofberg J., "YALMIP : a toolbox for modeling and optimization in MATLAB" presented at the 2004 IEEE International Conference on Robotics and Automation (IEEE Cat. No.04CH37508).(2004).
[41] Bai L., Jiang T., Li F. *et al.*, "Distributed energy storage planning in soft open point based active distribution networks incorporating network reconfiguration and DG reactive power capability", *Applied Energy,* 210(pp. 1082-1091 (2018).
[42] Li P., Ji H., Wang C. *et al.*, "Optimal Operation of Soft Open Points in Active Distribution Networks Under Three-Phase Unbalanced Conditions", *IEEE Transactions on Smart Grid,* 10(1), pp. 380-391 (2019).
[43] Wang J., Zhou N., Wang Q. *et al.*, "Hierarchically coordinated optimization of power distribution systems with soft open points and electric vehicles", *International Journal of Electrical Power & Energy Systems,* 149(pp. 109040 (2023).

Figure captions:

Table captions:

Figures:

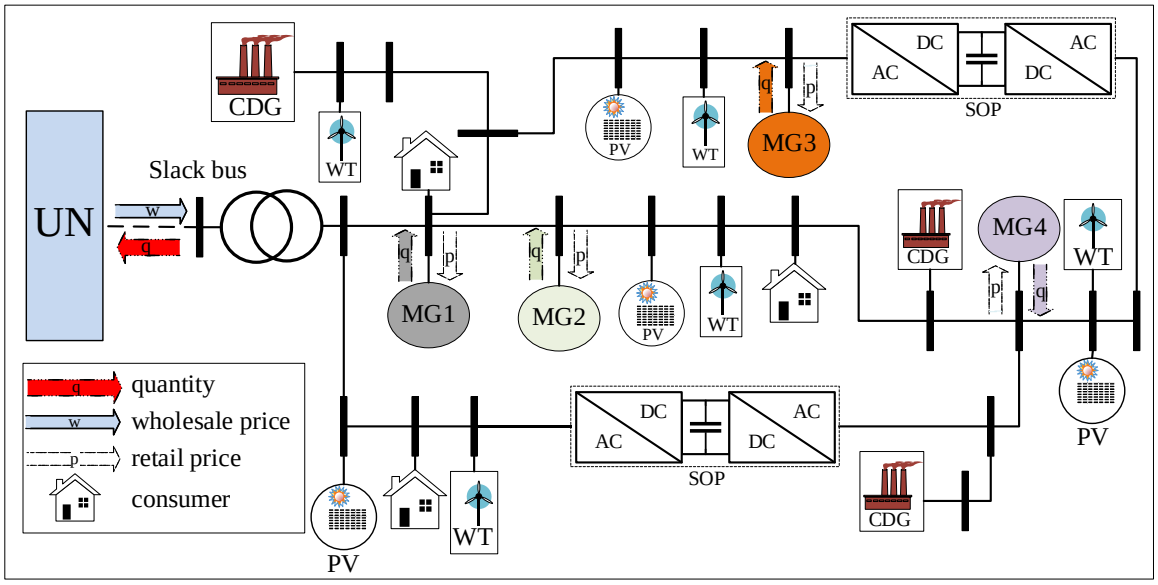

Fig. 1. An ADN with 4 connected MGs.

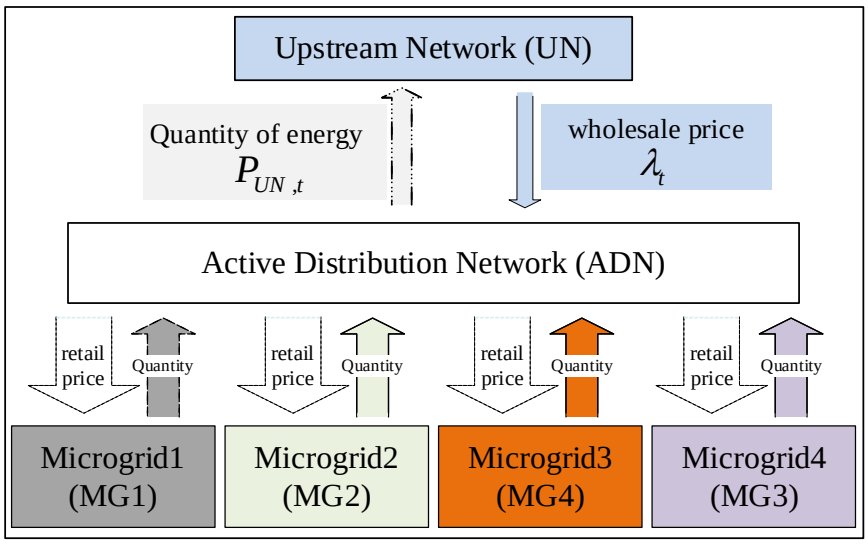

Fig. 2. Energy trading of ADN with MGs and UN.

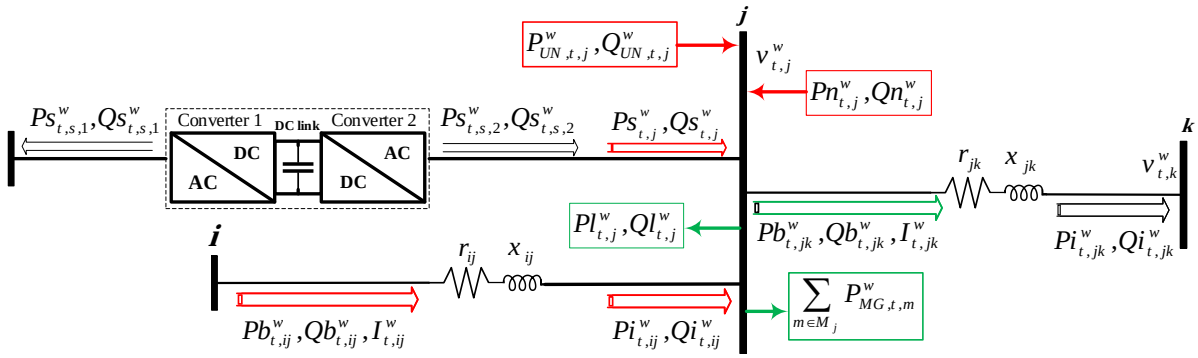

Fig. 3. The effect of SOPs on the ADN's power flow.

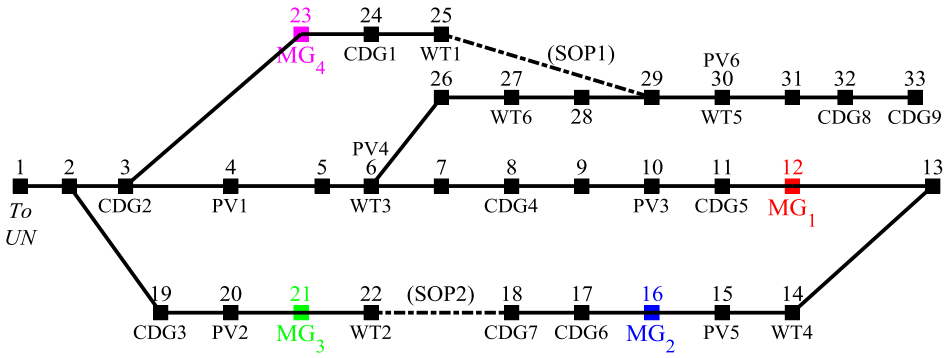

Fig. 4. One-line diagram of the case study.

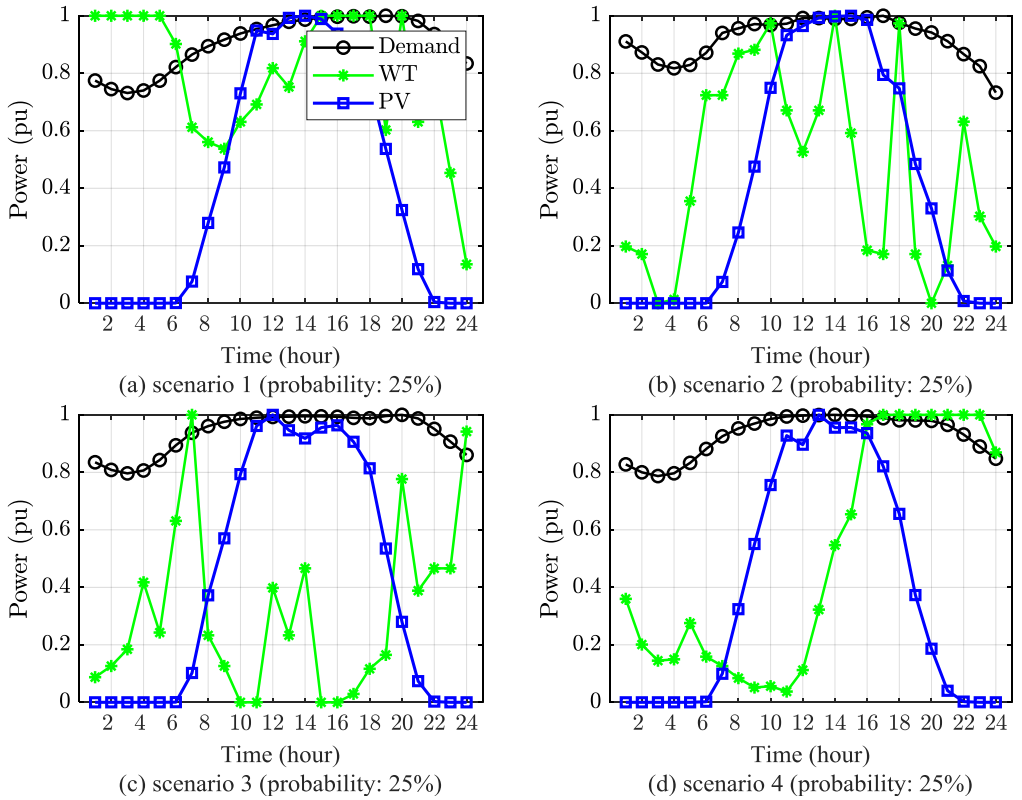

(a) scenario 1 (probability: 25%)

(b) scenario 2 (probability: 25%)

(c) scenario 3 (probability: 25%)

(d) scenario 4 (probability: 25%)

Fig. 5. The scenarios of demand, and PV and WT generation.

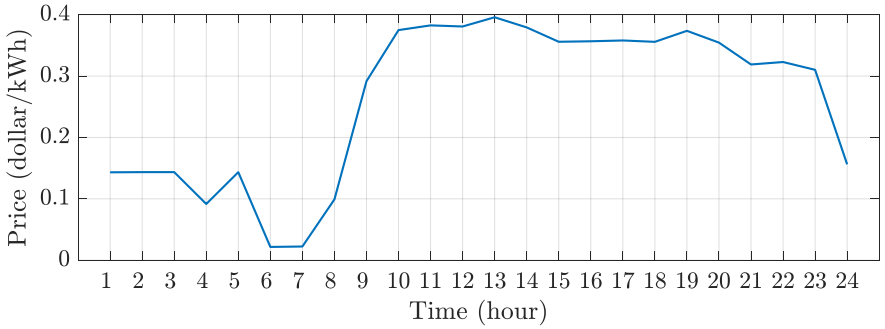

Fig. 6. The wholesale electricity price [37].

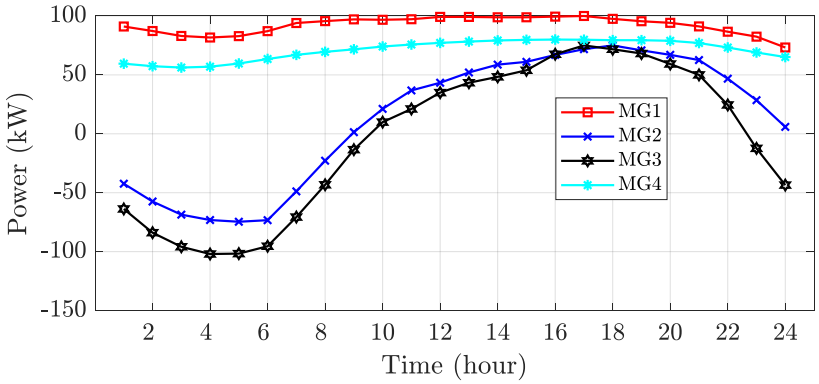

Fig. 7. The imported powers from the ADN (calculated by the MGs).

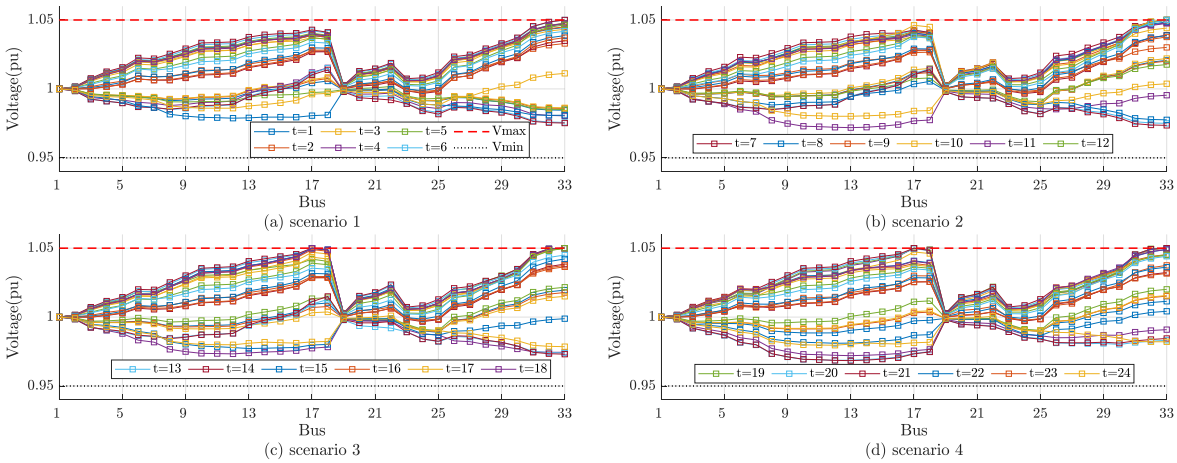

Fig. 8. The hourly voltage amplitude of the ADN, in scenarios: (a) 1, (b) 2, (c) 3, and (d) 4.

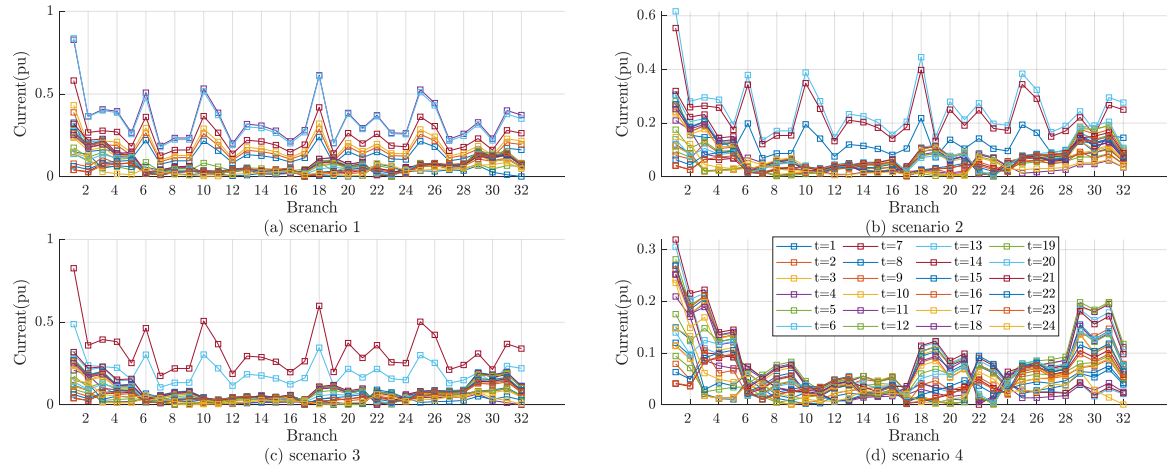

Fig. 9. The hourly current magnitude of the branches in all the scenarios.

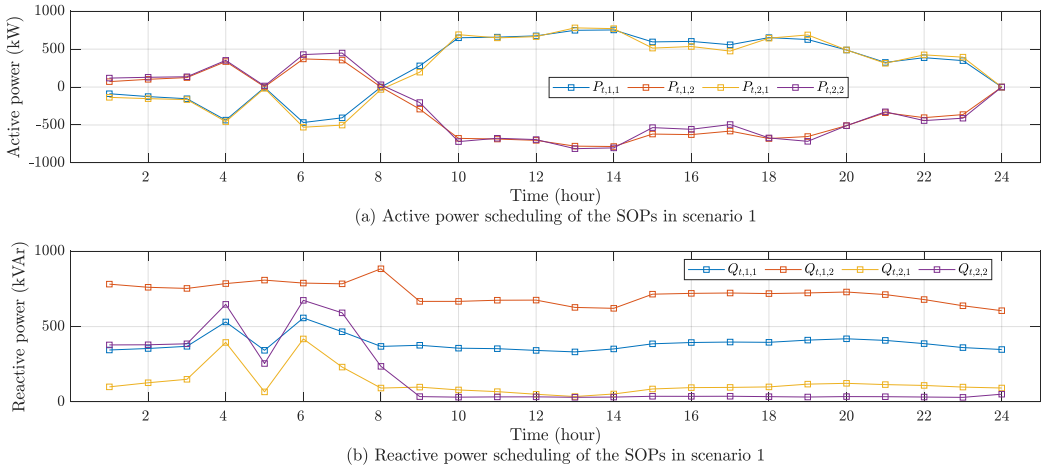

(a) Active power scheduling of the SOPs in scenario 1

(b) Reactive power scheduling of the SOPs in scenario 1

Fig. 10. The hourly active and reactive power injection scheduling of SOPs in scenario 1.

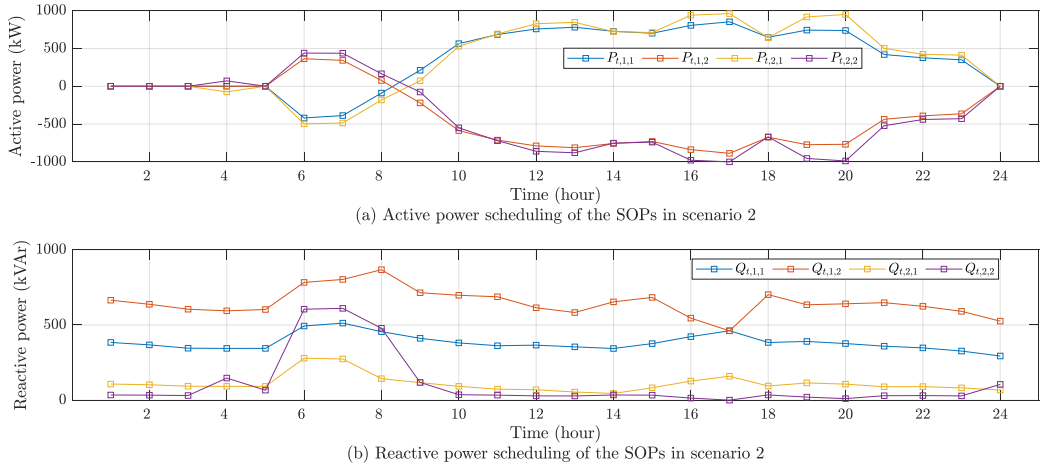

(a) Active power scheduling of the SOPs in scenario 2

(b) Reactive power scheduling of the SOPs in scenario 2

Fig. 11. The hourly active and reactive power injection scheduling of SOPs in scenario 2.

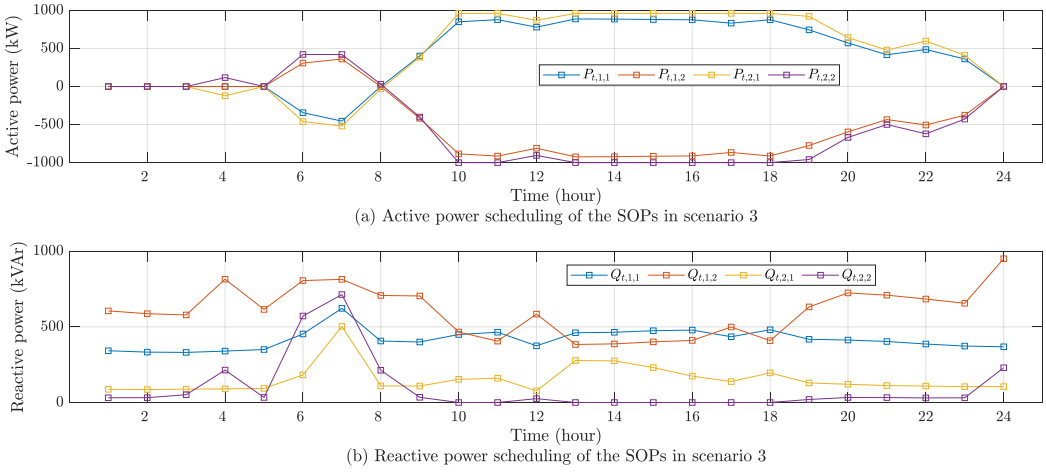

(a) Active power scheduling of the SOPs in scenario 3

(b) Reactive power scheduling of the SOPs in scenario 3

Fig. 12. The hourly active and reactive power injection scheduling of SOPs in scenario 3.

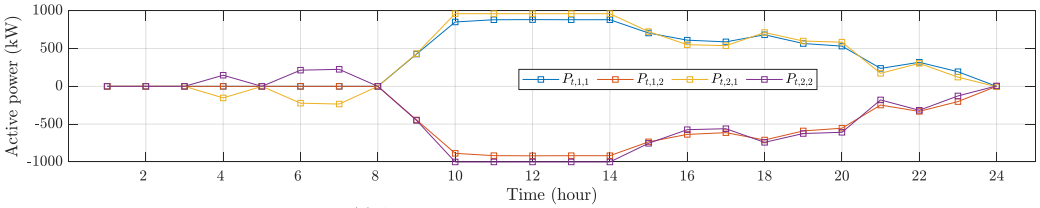

(a) Active power scheduling of the SOPs in scenario 4

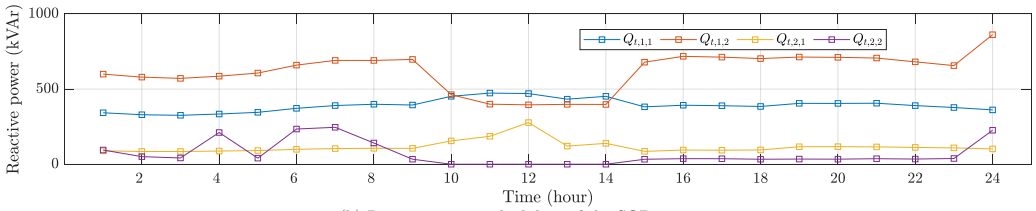

(b) Reactive power scheduling of the SOPs in scenario 4

Fig. 13. The hourly active and reactive power injection scheduling of SOPs in scenario 4.

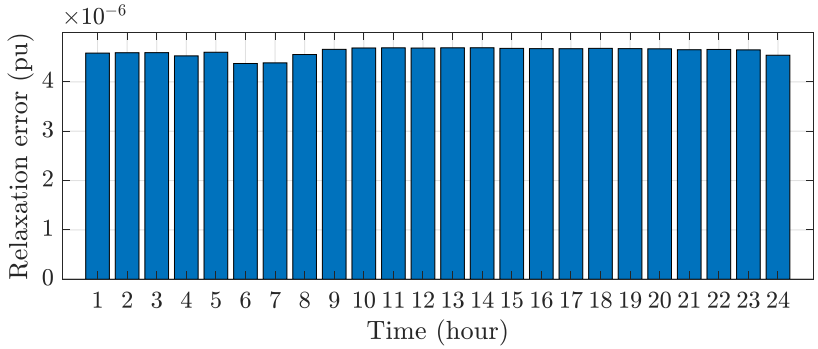

Fig. 14. The maximum error of the SOC relaxation in AC load flow constraint (27).

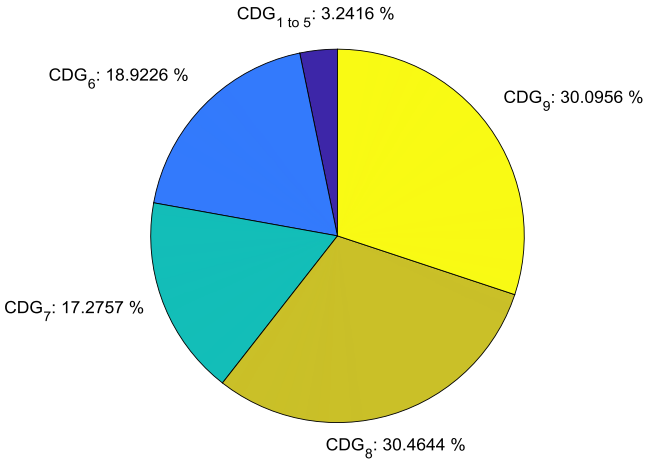

Fig. 15. pie chart of the total CDG generation.

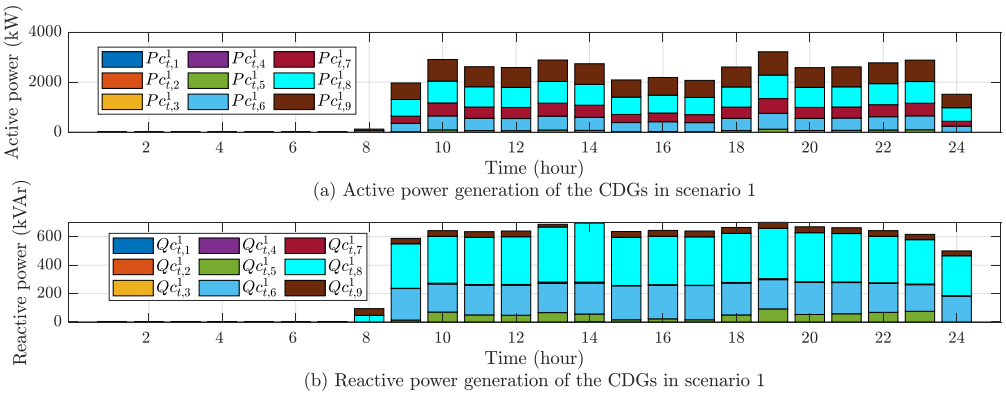

(a) Active power generation of the CDGs in scenario 1

(b) Reactive power generation of the CDGs in scenario 1

Fig. 16. The CDGs generation in scenario 1.

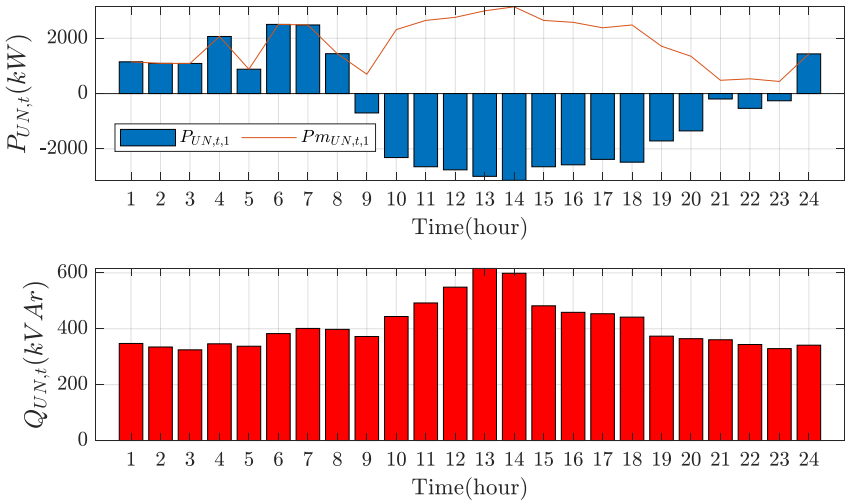

Fig. 17. The hourly imported power from the UN.

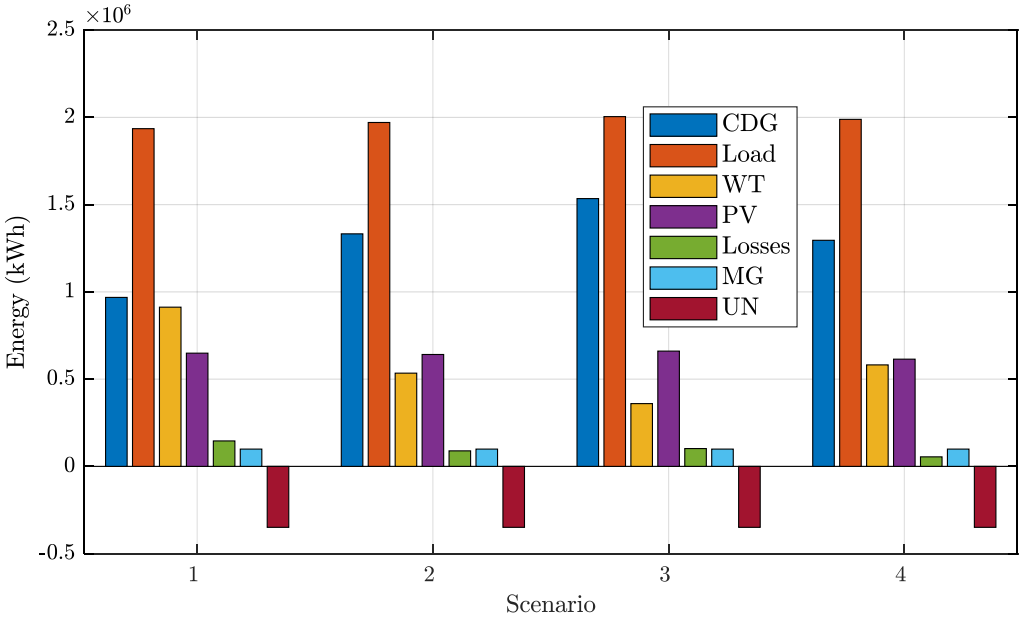

Fig. 18. Total energy dispatch of the ADN in different scenarios.

Tables:

Table 1. Comparing the capabilities of existing scheduling methods with the proposed method.

Ref	Type	Model	Power flow	Another agent		DERs modeling			Uncertainty		
				MG	UN	Renewables DG	CDGs	SOPs	Load	PV	WT
[9]	Scheduling	MISOCP	DISTFLOW	✓	✓	✓	✓	✓	×	×	×
[20]	Scheduling	MISOCP	DISTFLOW	✓	✓	✓	✓	Power loss ignored	×	×	×
[28]	Planning	MISOCP	Linearized Power flow	×	✓	✓	✓	✓	✓	×	✓
[41]	Planning	MISOCP	DISTFLOW	×	×	✓	✓	Power loss ignored	×	×	×
[42]	Scheduling	MISDP	branch flow	×	×	✓	×	✓	×	×	×
[43]	Scheduling	MILP	Linearized DistFlow	×	✓	×	×	✓	×	×	×
This paper	Scheduling	MISOCP	DISTFLOW	✓	✓	✓	✓	✓	✓	✓	✓

Table 2. Rated capacity of renewable DGs in the modified IEEE 33-bus ADN.

PV name	Rated capacity of PV (kW)	WT name	Rated capacity of WT (kW)
1	1000	1	250
2	500	2	250
3	500	3	500
4	200	4	500
5	200	5	250
6	300	6	250

Table 3. The energy losses of the ADN in various scenarios.

Scenario	**Energy losses of SOPs (kWh)**	**Energy losses of branches (kWh)**	**Total energy losses (kWh)**	**Share of SOP's losses (%)**
1	1325.267	4752.396	6077.663	21.806
2	1036.367	2670.295	3706.663	27.960
3	1201.600	3055.398	4256.998	28.226
4	790.761	1486.347	2277.108	34.727

Table 4. The hourly SOC relaxation error of AC load flow equation (27) in the modified IEEE 33-bus ADN.

Branch	$v_{t,i}^{w}$	$Pb_{t,ij}^{w}$	$Qb_{t,ij}^{w}$	$I_{t,ij}^{w}$	$I_{t,ij}^{w} \times v_{t,i}^{w}$	$Pb_{t,ij}^{w\ 2} + Qb_{t,ij}^{w\ 2}$	Error
1	1	0.143593	0.034121	0.021784	0.021784	0.021783	1.08E-06
2	0.998146	0.129983	0.02558	0.017578	0.017545	0.01755	4.54E-06
3	0.989369	0.057921	0.019707	0.003784	0.003743	0.003743	2.08E-07
4	0.986268	0.047664	0.012883	0.002472	0.002438	0.002438	2.09E-07
5	0.983691	0.04252	0.01031	0.001946	0.001914	0.001914	5.18E-08
6	0.978444	0.055416	0.021054	0.003592	0.003515	0.003514	4.88E-07
7	0.97553	0.038424	0.01244	0.001672	0.001631	0.001631	1.12E-08
8	0.965436	0.021295	0.003836	0.000485	0.000468	0.000468	2.96E-08
9	0.962348	0.016179	0.002119	0.000277	0.000266	0.000266	5.07E-08
10	0.960127	0.011076	0.000411	0.000128	0.000123	0.000123	4.87E-07

11	0.959852	0.007261	-0.00213	5.99E-05	5.75E-05	5.73E-05	2.35E-07
12	0.959546	-0.00515	-0.0051	5.48E-05	5.25E-05	5.25E-05	2.89E-10
13	0.961225	-0.01024	-0.00807	0.000177	0.00017	0.00017	1.09E-07
14	0.962636	0.023039	-0.01486	0.000781	0.000752	0.000752	1.01E-07
15	0.961914	0.017925	-0.01573	0.000591	0.000569	0.000569	6.49E-08
16	0.961316	0.012226	-0.01745	0.000472	0.000454	0.000454	7.82E-09
17	0.963105	0.007103	-0.01919	0.000435	0.000419	0.000419	7.23E-08
18	0.998146	0.005009	0.003392	3.73E-05	3.72E-05	3.66E-05	6.39E-07
19	0.997977	-0.00262	1.17E-06	6.88E-06	6.87E-06	6.86E-06	1.14E-08
20	0.998468	-0.01025	-0.00339	0.000117	0.000117	0.000116	1.81E-07
21	0.999195	-0.01352	-0.00678	0.000229	0.000229	0.000229	9.4E-08
22	0.989369	0.063894	0.002207	0.004131	0.004087	0.004087	1.56E-07
23	0.985691	0.049635	-0.00211	0.002504	0.002468	0.002468	4.07E-08
24	0.980329	0.013899	-0.01917	0.000572	0.000561	0.000561	4.36E-08
25	0.978444	0.025378	-0.01252	0.000819	0.000801	0.000801	4.53E-07
26	0.977963	0.020282	-0.01465	0.00064	0.000626	0.000626	3.04E-07
27	0.977509	0.036915	-0.01677	0.001682	0.001644	0.001644	2.97E-08
28	0.974598	0.031719	-0.01857	0.001386	0.001351	0.001351	5.32E-08
29	0.973044	0.021479	0.061629	0.004378	0.00426	0.004259	1.24E-07
30	0.969701	0.026119	0.010707	0.000822	0.000797	0.000797	3.86E-08
31	0.965245	0.013356	0.004725	0.000208	0.000201	0.000201	2.45E-07
32	0.964514	0.00032	-0.00018	7.34E-07	7.08E-07	1.35E-07	5.73E-07

Table 5. The detailed operation cost of the ADN in various scenarios.

Scenario	C_{UN} (\$)	C^{w}_{CDG} (\$)	C^{w}_{l} (\$)	C^{w}_{ls} (\$)	C^{w}_{lB} (\$)	C^{w}_{to} (\$)
1	-9273.86	8314.514	949.5775	290.7774	658.8001183	-9.77381
2	-9273.86	12024.03	798.6684	295.6856	502.982855	3548.838
3	-9273.86	14749.36	918.7104	341.4753	577.2350816	6394.205
4	-9273.86	11527.22	755.1624	280.4742	474.6881223	3008.515

Table 6. Comparison of operating costs in two cases with and without SOPS.

Scenario	C_{UN} (\$)		C^{w}_{CDG} (\$)		C^{w}_{l} (\$)		C^{w}_{to} (\$)	
	with SOPs	without SOPs	with SOPs	without SOPs	with SOPs	without SOPs	with SOPs	without SOPs
1	-9273.87	-1972.09	8314.514	4444.017	949.577	257.975	-9.774	2729.9
2	-9273.87	-1972.09	12024.04	10223.35	798.668	242.29	3548.838	8493.543
3	-9273.87	-1972.09	14749.36	14284.48	918.71	202.933	6394.205	12515.32
4	-9273.87	-1972.09	11527.22	9913.427	755.162	228.517	3008.515	8169.851

Biographies

Pezhman Khalouie completed her B.Sc study in power engineering at Islamic Azad University - Tabriz Branch in 2011 and her M.Sc study in power engineering at Islamic Azad University – Science and research Branch. He is currently a PhD student at the Islamic Azad University - Urmia Branch. The main objective of her PhD thesis is decentralized framework for day-ahead scheduling of multi-area active distribution network in the presence of soft open points.

Payam Alemi has several years' experience on design and control of power converters. The analysis and control of grid-connected multilevel T-type three-level AC/DC/AC voltage source converters by utilizing new RB-IGBT Module from Fuji Electronic Company and novel high-voltage film capacitors in the converter DC-link was proposed. The topology design, simulation, and also assembling of the converter was done completely for experimental study in Yeungnam University, South Korea during his PhD.

Mojtaba Beiraghi received the Ph.D. degree in power engineering from Sharif University in 2016. He design a power system stabilizer to mitigate oscillations between different regions of the power system using wide-area measurements during his PhD.